Cell Reports
Report

Cell PRESS
Open ACCESS

RBMX: A Regulator for Maintenance and Centromeric Protection of Sister Chromatid Cohesion

Sachihiro Matsunaga,[1,2,4,*] Hideaki Takata,[1,4] Akihiro Morimoto,[1,4] Kayoko Hayashihara,[1,5] Tsunehito Higashi,[2] Kouhei Akatsuchi,[1] Eri Mizusawa,[1] Mariko Yamakawa,[1] Mamoru Ashida,[1] Tomoko M. Matsunaga,[2] Takachika Azuma,[3] Susumu Uchiyama,[1] and Kiichi Fukui[1,*]

[1]Department of Biotechnology, Graduate School of Engineering, Osaka University, Suita 565-0871, Japan
[2]Department of Applied Biological Science, Faculty of Science and Technology, Tokyo University of Science, 2641 Yamazaki, Noda, Chiba 278-8510, Japan
[3]Division of Biosignaling, Research Institute for Biological Sciences, Tokyo University of Science, 2669 Yamazaki, Noda, Chiba 278-0022, Japan
[4]These authors contributed equally to this work
[5]Present address: Institute for Protein Research, Osaka University, 3-2 Yamadaoka, Suita, Osaka 565-0871, Japan
*Correspondence: sachi@rs.tus.ac.jp (S.M.), kfukui@bio.eng.osaka-u.ac.jp (K.F.)
DOI 10.1016/j.celrep.2012.02.005

SUMMARY

Cohesion is essential for the identification of sister chromatids and for the biorientation of chromosomes until their segregation. Here, we have demonstrated that an RNA-binding motif protein encoded on the X chromosome (RBMX) plays an essential role in chromosome morphogenesis through its association with chromatin, but not with RNA. Depletion of RBMX by RNA interference (RNAi) causes the loss of cohesin from the centromeric regions before anaphase, resulting in premature chromatid separation accompanied by delocalization of the shugoshin complex and outer kinetochore proteins. Cohesion defects caused by RBMX depletion can be detected as early as the G2 phase. Moreover, RBMX associates with the cohesin subunits, Scc1 and Smc3, and with the cohesion regulator, Wapl. RBMX is required for cohesion only in the presence of Wapl, suggesting that RBMX is an inhibitor of Wapl. We propose that RBMX is a cohesion regulator that maintains the proper cohesion of sister chromatids.

INTRODUCTION

Authentic construction of the chromosome structure consisting of two sister chromatids, named cohesion, is required for faithful transmission of the genomic DNA to the daughter cells (Nasmyth and Haering, 2009). The genomic DNA is duplicated in the S phase, and sister chromatid cohesion is regulated by a cohesin complex consisting of Scc1 (Rad21), Scc3 (also known as SA1 and SA2 in vertebrates), Smc1, and Smc3 (Nasmyth, 2001; Koshland and Guacci, 2000; Losada and Hirano, 2005). The loading of cohesin onto chromatin occurs early in the G1 phase (Losada, 2008; Peters et al., 2008). Cohesion is established by the family of Eco1 cohesin acetyltransferases that acetylate Smc3 during the S phase (Ivanov et al., 2002; Rowland et al., 2009). The acetylation of Smc3 is necessary for Sororin recruitment to chromatin-bound cohesin complexes in mammalian cells (Lafont et al., 2010; Nishiyama et al., 2010). This process is thought to be essential for the maintenance of cohesion during the S/G2 phase. During mitosis in mammalian cells, cohesion dissolution is performed via two pathways. One is the prophase pathway in which a mitotic kinase polo-like kinase 1 (Plk1) phosphorylates SA2 and disassociates the cohesin complex along the chromosome arm (Sumara et al., 2002; Hauf et al., 2005). The centromeric cohesion between sister chromatids must be maintained and protected from Plk1 until metaphase. The remaining cohesion in the centromeric region is sufficient to allow proper chromosome alignment and timely segregation (Losada, 2008; Peters et al., 2008). The other pathway involves the separase-mediated cleavage of Scc1 after securin degradation by the anaphase-promoting complex (APC) (Nasmyth, 2002). Recent studies have revealed that the shugoshin (Sgo) complex containing Sgo1 and protein phosphatase 2A (PP2A) protects the centromeric cohesin until the onset of anaphase (Watanabe, 2005; Kitajima et al., 2006; Rivera and Losada, 2006; Tang et al., 2006). PP2A recruited by Sgo1 can dephosphorylate SA2 that has been phosphorylated by Plk1. Thus, the depletion of Sgo1 or PP2A results in the loss of cohesin at centromeres, leading to premature sister chromatid separation (Kitajima et al., 2006; Tang et al., 2006). The recruitment of the Sgo complex to centromeric regions depends on a heterochromatic protein HP1α and the phosphorylation of H2A by a protein kinase Bub1 (Yamagishi et al., 2008; Kawashima et al., 2010).

To further elucidate the chromosome morphogenesis, we performed functional analyses of chromosome proteins that have been identified previously by the proteome analysis of human chromosomes (Uchiyama et al., 2005; Takata et al., 2007c). We found an *R*NA-*b*inding *m*otif protein encoded on the *X* chromosome (RBMX) as a chromosomal protein. RBMX was identified as a paralog of a Y chromosome-linked gene, RBMY, which is responsible for spermatogenesis (Delbridge et al., 1999; Mazeyrat et al., 1999) and which has been associated with the activation of liver cancers (Tsuei et al., 2004). RBMX belongs to the hnRNP family of proteins that have a highly conserved RNA-binding domain and are responsible for pre-mRNA splicing (Heinrich et al., 2009). Its

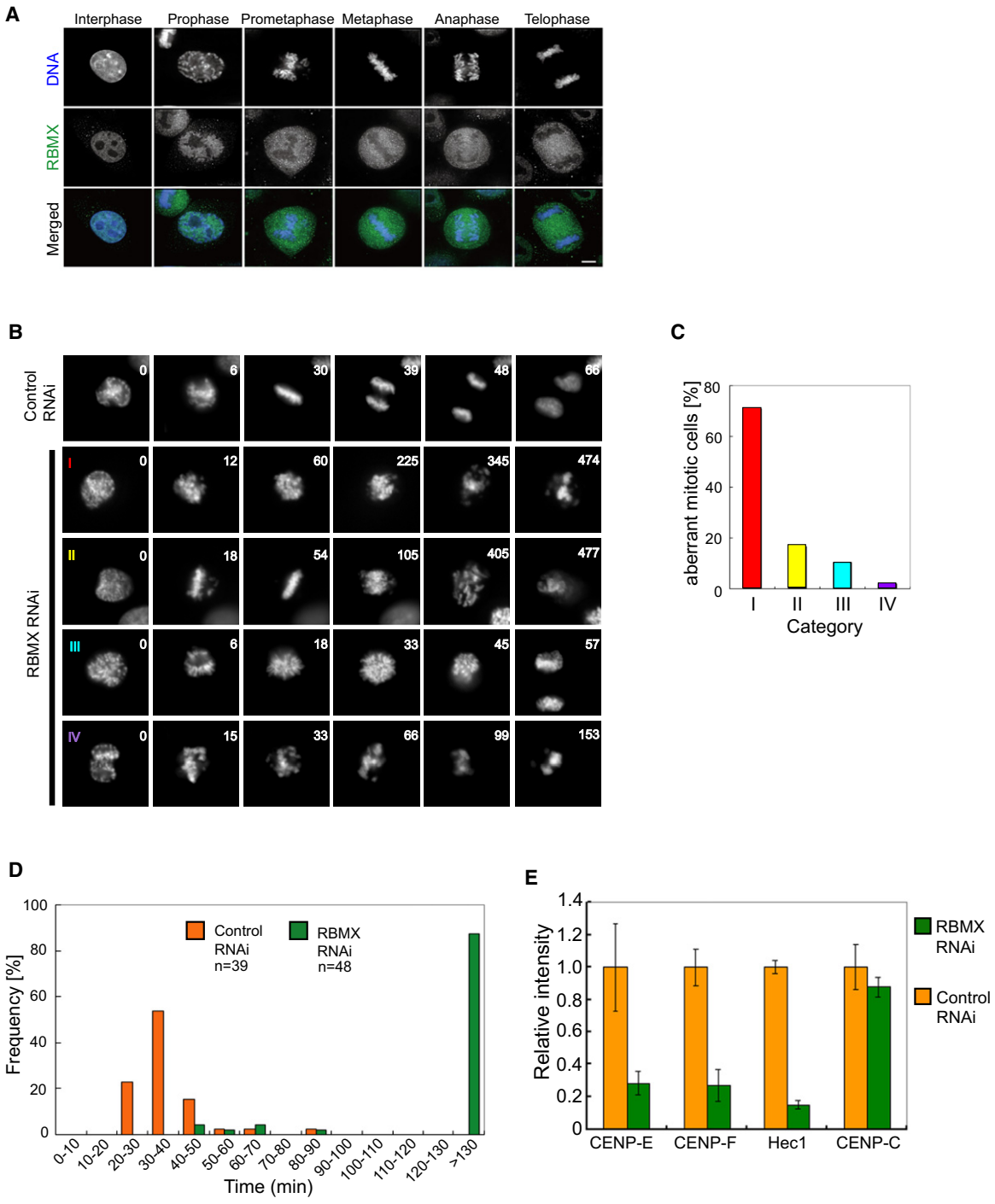

Figure 1. Localization of RBMX and Mitotic Progression Defect

(A) HeLa cells were stained with anti-RBMX antibody (green). DNA was stained with Hoechst 33342 (blue). Deconvolution processing was performed on all images. Scale bar, 5 μm.

(B) RBMX was depleted in HeLa cells stably expressing GFP-H1.2. The number (top right) in each panel shows the time point (min) after nuclear envelope breakdown (NEBD). In RBMX-depleted cells, four types of aberrant chromosome dynamics (I–IV) were observed: I, chromosomes never formed the distinct metaphase plate and were scattered throughout the cytoplasm; II, chromosomes were aligned at the metaphase plate but began to scatter throughout the cytoplasm after a long arrest at metaphase; III, chromosomes were segregated without alignment at the metaphase plate; and IV, chromosomes were decondensed in early mitosis, and the cell became apoptotic.

(C) Frequencies of the four types of aberration of chromosome dynamics in RBMX RNAi cells. Categories I–IV correspond to the numerals indicated in (B).

ubiquitous expression in almost all organs indicates that RBMX has essential functions in various cellular processes. The in vivo function of RBMX is currently unknown; however it has been reported to be required for brain development and has been implicated to have a relationship with systemic lupus erythematosus (Tsend-Ayush et al., 2005; Soulard et al., 2002). Here, we demonstrate that RBMX plays crucial roles in the maintenance and centromeric protection of sister chromatid cohesion.

RESULTS AND DISCUSSION

Depletion of RBMX Inhibits Chromosome Congression

To evaluate the mitotic function, we first examined the localization of RBMX in HeLa cells throughout the cell cycle. At interphase, RBMX was localized in the nucleoplasm except for in the nucleoli (Figure 1A). After the onset of mitosis, RBMX started to dissociate from the chromosomes to the cytoplasm and was distributed throughout the cytoplasm at prometaphase. Western blotting using synchronized cells with double-thymidine treatment and subsequent addition of nocodazole showed that the RBMX expression level was constant throughout the cell cycle (see Figure S1A).

To examine the function of RBMX in chromosome dynamics, we performed RNA interference (RNAi)-mediated depletion of RBMX. The expression of RBMX significantly decreased (by over 60%) after 48 hr of transfection of HeLa cells with two different RBMX-specific siRNAs, siRNA-1 or siRNA-2 (Figures S1B and S1F). There were no significant differences in the knockdown phenotypes between the two RNAi experiments with different siRNAs (Figures S1C, S1D, S2B, and S2C); siRNA-1 was used for further studies of RBMX. The depletion of RBMX resulted in the accumulation of mitotic cells by longtime arrest at prometaphase. The reduction of RBMX frequently caused defects in chromosome alignment. Although chromosome condensation occurred in the normal way in RBMX-depleted cells, chromosome alignment at the metaphase plate was significantly impaired (Figure 1B). Nonaligned chromosomes (when more than ten chromosomes were not aligned at the metaphase plate or when chromosomes were scattered throughout the cytoplasm) were frequently observed in RBMX-depleted cells (76.8% of mitotic cells). Misaligned chromosomes (when most of the chromosomes were aligned at the metaphase plate, but one to ten chromosomes were not aligned) were also observed in 5.2% of RBMX-depleted mitotic cells. Chromosomal defects like these were rarely observed in the control cells (misaligned, 1.6%; nonaligned, 0.9%). The expression levels of cyclin B1, which is degraded at anaphase, were the same in the RBMX-depleted cells and in the control metaphase cells (Figure S1E). The expression level of securin increased in the RBMX-depleted cells (Figure S1F). Furthermore, inhibition of APC/C activity using MG132 did not decrease the defect in chromosome congression (Figure S1G). These results indicate that these chromosomal defects were generated before anaphase. The expression levels of Sororin, Scc1, Sgo1, tri-methylated K9 of histone H3, Bub1, BubR1, HP1α, Plk1, and Mad2 were the same in the RBMX-depleted cells and in the control cells (Figures S1F and S1H–S1J).

To investigate the effects of RBMX depletion on chromosome dynamics in living cells, we performed time-lapse observations of GFP-histone H1.2 in RBMX-depleted HeLa cells (Gambe et al., 2007). We found that 87.5% of the RBMX-depleted cells remained from prometaphase to metaphase for more than 130 min, whereas in control RNAi cells, chromosome alignment occurred about 30 min after the nuclear envelope breakdown (Figures 1B and 1D). Chromosome alignment defects and arrest in prometaphase were the highest frequency defects (Figure 1C). Consistent with the observations in fixed cells (Figures 1A and S1C), chromosome condensation occurred appropriately, but chromosome congression was severely affected in RBMX-depleted cells. Moreover, we found that the expression of RNAi-refractory RBMX reduced the percentage of congression defects in RBMX RNAi cells (Figure S1D). This observation shows that the congression defects in mitotic chromosomes were the direct result of RBMX repression by RNAi. Thus, we have shown that RBMX can play an important role in mitotic progression before chromosome alignment.

Microtubule attachment to kinetochores and the formation of stable kinetochore fibers are essential for chromosome alignment (Kline-Smith and Walczak, 2004). Therefore, we analyzed the localization of the outer kinetochore components, CENP-E, CENP-F, Hec1, and Mis13 (Cheeseman and Desai, 2008; Obuse et al., 2004), by immunostaining. The two distinct signals from these proteins were detected outside the CREST signals on individual chromosomes in the control cells (Figures S1K–S1N). In RBMX-depleted cells the signals from these proteins decreased to less than 30% of the signals in the control cells (Figures 1E and S1K–S1N). In contrast to the outer kinetochore proteins, the signal intensities from the inner kinetochore proteins, CENP-A and CENP-C, were not changed by RBMX depletion (Figures 1E and S1O). The degeneration of the outer kinetochore structure that is indicated by this result might induce defects in chromosome alignment because microtubule attachment to the kinetochores is impaired.

RBMX Associates with Chromatin in an RNA-Independent Manner

We next investigated which domains of RBMX might be essential for normal mitotic progression. We defined three characteristic domains in RBMX: RRM, the RNA recognition motif; SRR, a serine and arginine-rich region; and TRR, a tyrosine-rich region (Figure 2A). To investigate the possible role of each of these domains, we constructed four rescue vectors encoding GFP-tagged RNAi-refractory full-length RBMX (Full-r) and RBMX

(D) The time intervals between NEBD and the onset of anaphase were measured in live-cell imaging of control and RBMX RNAi cells. RBMX-depleted cells showed a significant delay in the onset of anaphase.

(E) Changes in the localization of outer kinetochore proteins. After immunostaining of CENP-E, CENP-F, Hec1, and CENP-C, the fluorescence intensities of each protein were quantified. ($n > 3$; mean values and SD are shown). Error bars represent SD in triplicate experiments.

See also Figure S1.

Cell PRESS
Open ACCESS

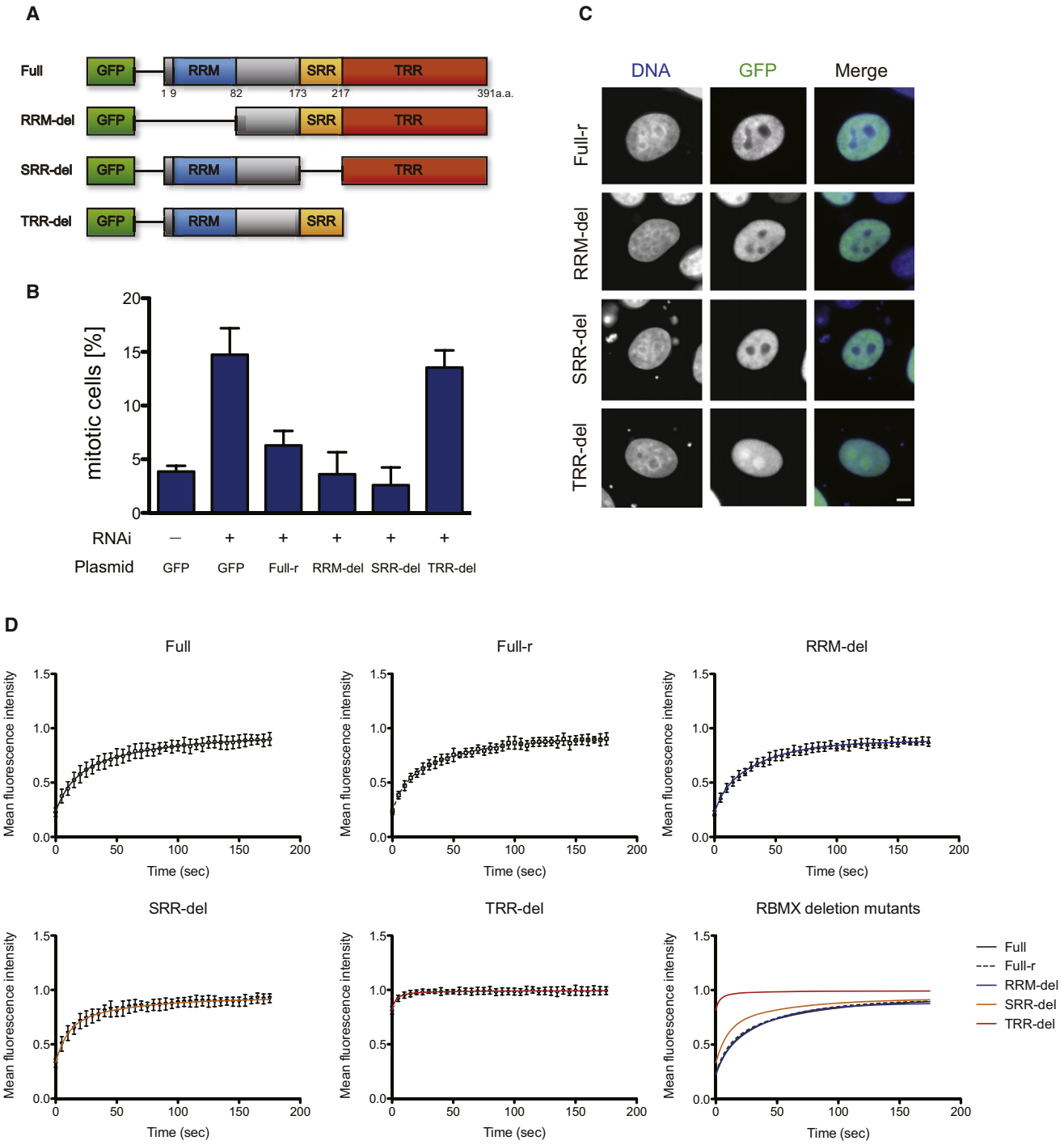

Figure 2. Domain Analyses of RBMX

(A) Domain structure of RBMX.

(B) Mitotic index was calculated after immunostaining with anti-GFP and anti-α-tubulin antibodies. HeLa cells were transfected with RNAi-refractory GFP-tagged RBMX deletion mutants and were subsequently transfected with RBMX siRNA. Error bars represent SD in triplicate experiments.

(C) Localization of RBMX deletion mutants. HeLa cells transiently expressing GFP-tagged RBMX deletion mutants were fixed with 4% PFA and immunostained with anti-GFP antibody. Scale bar, 5 μm.

(D) Fluorescence recovery of RBMX deletion mutants was monitored and quantified. Lines represent the best-fitting curves for the individual data sets. ($n \geq 10$; mean values and SD are shown).

See also Figure S2.

deletion mutants (RRM-del, SRR-del, and TRR-del). Next, we transfected HeLa cells, first with the rescue vectors and then with RBMX siRNA. Forty-eight hours after the second transfection, we found that Full-r and two of the deletion mutants, RRM-del and SRR-del, could rescue the accumulation of mitotic cells induced by RBMX depletion. In contrast, TRR-del did not reduce the percentage of accumulated mitotic cells (Figure 2B). This result suggested that the TRR domain is important for normal mitotic progression.

To gain more insight into the functions of these domains, we observed the localization patterns of the RBMX deletion mutants. HeLa cells transiently expressing the deletion mutants were immunostained with anti-GFP antibody. Immunostaining analysis showed that similarly to the intact RBMX, Full-r, RRM-del, and SRR-del were localized throughout the nucleoplasm excluding the nucleoli (Figure 2C). TRR-del, on the other hand, was localized in the nucleoli in addition to in the nucleoplasm (Figure 2C), whereas a TRR-only protein (a GFP-tagged TRR protein) was localized in the nucleoplasm excluding the nucleoli (Figure S2A). These results clearly imply that the TRR domain of RBMX was responsible for either nucleoplasm retention or nucleoli exclusion.

To further confirm this result, we analyzed the mobility of the RBMX deletion mutants using fluorescence recovery after photobleaching (FRAP). A part of the nucleus was photobleached, and the redistribution of GFP signals in the photobleached region was monitored and quantified. We found that the mobility of RRM-del was the same as that of intact RBMX and Full-r (Figure 2D). This result and the results of the rescue experiment together strongly suggest that RNA-binding ability mediated by the RRM domain is dispensable, not only for normal chromosome congression in mitosis but also for the stable association of RBMX with chromatin in interphase. Interestingly, TRR-del showed much faster recovery than the other deletion mutants, possibly because it diffused in the nucleus (Figure 2D), suggesting that the TRR domain is essential for the stable binding of RBMX to chromatin. These results indicate that the association of RBMX with chromatin and its function in mitotic progression are not dependent on its RNA-binding ability via the RRM domain.

RBMX Regulates the Centromeric Localization of the Sgo Complex

To examine the effect of RBMX depletion on chromosome structure, we prepared metaphase chromosome spreads from both control and RBMX RNAi cells (Figure 3A). We observed the following four morphologies (Figure 3B): closed arm, open arm, mild separation, and complete separation. In control cells, 79% of prometaphase chromosomes showed open arm chromosomes, and mild and complete separation morphologies were rarely observed (Figure 3B). In contrast when siRNA-1 was used in RBMX-depleted cells, sister chromatids were drastically separated (mild separation, 2%; complete separation, 94%) (Figure 3B). A similar phenotype was observed when siRNA-2 was used (Figures S2B and S2C). These results indicate that depletion of RBMX caused loss of sister chromatid cohesion. The chromatid separation caused by RBMX depletion was rescued by exogenous expression using the Full-r vector (Figure 3B). Neither the TRR-del vector nor a vector with only the TRR domain could suppress the chromatid separation (Figures S2 and S2C). This result suggests that the TRR domain is necessary but not sufficient for RBMX's role in cohesion.

Chromatid separation depends on the removal of cohesin with Plk1. Indeed, 94% of Plk1-depleted cells exhibited closed arm chromosomes (Figure 3B) as was previously reported (Giménez-Abián et al., 2004). When double knockdown of RBMX and Plk1 was performed, precocious chromatid separation was dramatically diminished compared to what was observed in RBMX-depleted cells (Figure 3B). These results indicate that centromeric cohesin was inappropriately removed with Plk1 in RBMX-depleted cells. Subsequently, we investigated the localization of Sgo1 and one of the PP2A subunits (B56α) after RBMX RNAi. In control cells the signals from Sgo1 and B56α were detected between paired kinetochores visualized by the kinetochore marker CREST during prometaphase (Figures 3C and 3D). In RBMX-depleted cells, single intense CREST signals were detected from scattered chromatids, demonstrating that the sister chromatids were unpaired. Signals from Sgo1 and B56α could not be detected from the separated chromatids, indicating that RBMX was required for centromeric localization of the Sgo complex. In RBMX-depleted cells, centromeric cohesin signals were not detected (Figure 3E), although the expression level of Scc1 was unchanged compared to the control (Figure S1H). Scc1 depletion did not induce the reduction of outer kinetochore proteins (Figures S3A–S3C) as was previously reported (Vagnarelli et al., 2004), suggesting that the displacement of outer kinetochore components might not be directly attributed to the absence of Sgo complex. Moreover, we could not detect centromeric localization of Sgo1 in RBMX/Plk1 double-knockdown cells (Figure 3F). The percentage of closed arm chromosomes in RBMX/Plk1 double-knockdown cells was comparable to their percentage in Plk1 knockdown cells (Figure 3B). However, the elimination of Sgo1 from centromeric regions was caused specifically by depletion of RBMX, indicating that precocious sister chromatid separation was caused by the loss of cohesin at centromeres. Because Aurora B activity has also been implicated in the removal of cohesin from chromosome arms (Losada et al., 2002; Dai et al., 2006; Salic et al., 2004), we also investigated the effect of Aurora B depletion in RBMX RNAi cells. Depletion of Aurora B increased the percentage of closed arm phenotype in spread chromosomes (Figure 3B). Additionally, Aurora B depletion could rescue the chromatid separation phenotype observed in RBMX-depleted cells. These results suggest that RBMX is essential for centromeric localization of Sgo1, and that Plk1 and Aurora B are required for sister chromatid separation in RBMX-depleted cells.

RBMX Is Required for Cohesin Maintenance

Of RBMX/Plk1 double-knockdown cells, 19% exhibit mild and complete separation morphologies (Figure 3B), suggesting that RBMX reduction impairs cohesion maintenance before the prophase pathway. In support of this hypothesis, FISH experiments in G2 cells released from a thymidine block revealed that paired chromatids in RBMX-depleted cells at the G2 phase were more distantly located than in control cells (Figure 4A). Of RBMX-depleted cells, 31% showed distances that were outside

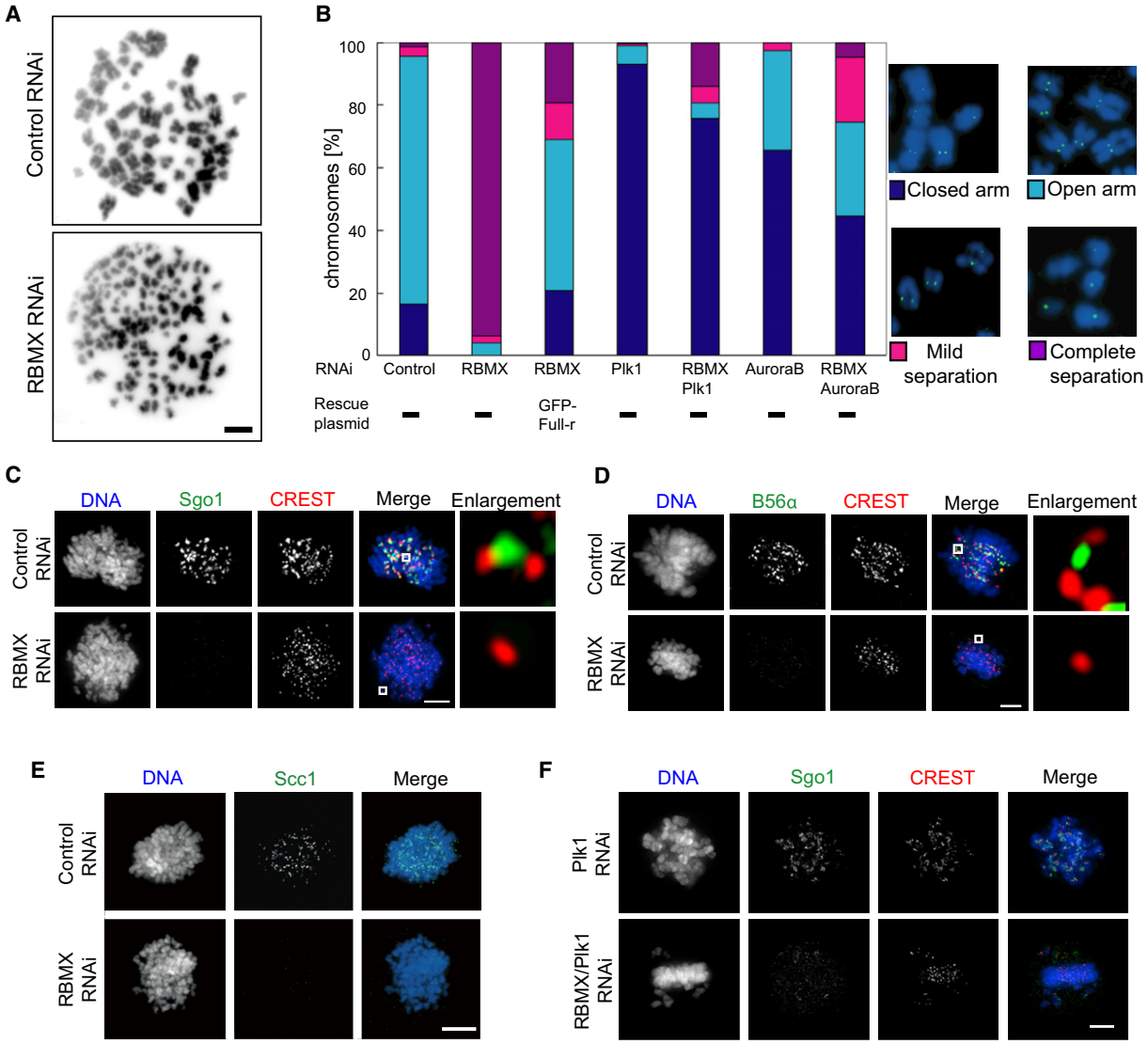

Figure 3. RBMX Functional Analyses in Chromosome Construction

(A) Chromosome morphology in control and in RBMX-depleted cells. Cells were synchronized at mitosis using 0.1 μg/ml colcemid for 3 hr, and spread on a glass slide using Cytospin. Chromosomes were visualized with DAPI. Scale bar, 5 μm.

(B) Chromosome morphologies were categorized into four groups: closed arm, chromosomes maintained sister chromatid cohesion over their entire length; open arm, sister chromatids cohered at the centromeric region, but not along the chromosome arm; mild separation, sister chromatids were partially separated, and their cohesion was maintained at the centromere or on the chromosome arm, and primary constriction was not observed at the centromere; and complete separation, sister chromatids were completely separated. DNA was stained with DAPI (blue), and kinetochores were visualized with CENP-A (green). Values were derived from more than 57 cells in 3 independent experiments.

(C) RBMX knockdown cells were immunostained with anti-Sgo1 antibody (green) and anti-CREST serum (red). Enlargement shows an example of the centromeric region. Scale bar, 5 μm.

(D) RBMX knockdown cells were immunostained with anti-B56α antibody (green) and anti-CREST serum (red). Enlargement shows an example of the centromeric region. Scale bar, 5 μm.

(E) RBMX knockdown cells were immunostained with anti-Scc1 (green) antibody. Scale bar, 5 μm.

(F) Plk1 knockdown, and RBMX and Plk1 double-knockdown cells were immunostained with anti-Sgo1 antibody (green) and anti-CREST serum (red). Scale bar, 5 μm.

See also Figure S3.

the range of the distances in control cells. These data suggest that RBMX depletion induced a partial premature resolution or abnormal association of the sister chromatids, resulting in the failure in proper cohesion between sister chromatids. To confirm the chromatin association of RBMX, cell lysates of synchronized cells at S or G2 phase were separated into cytoplasmic, nuclear,

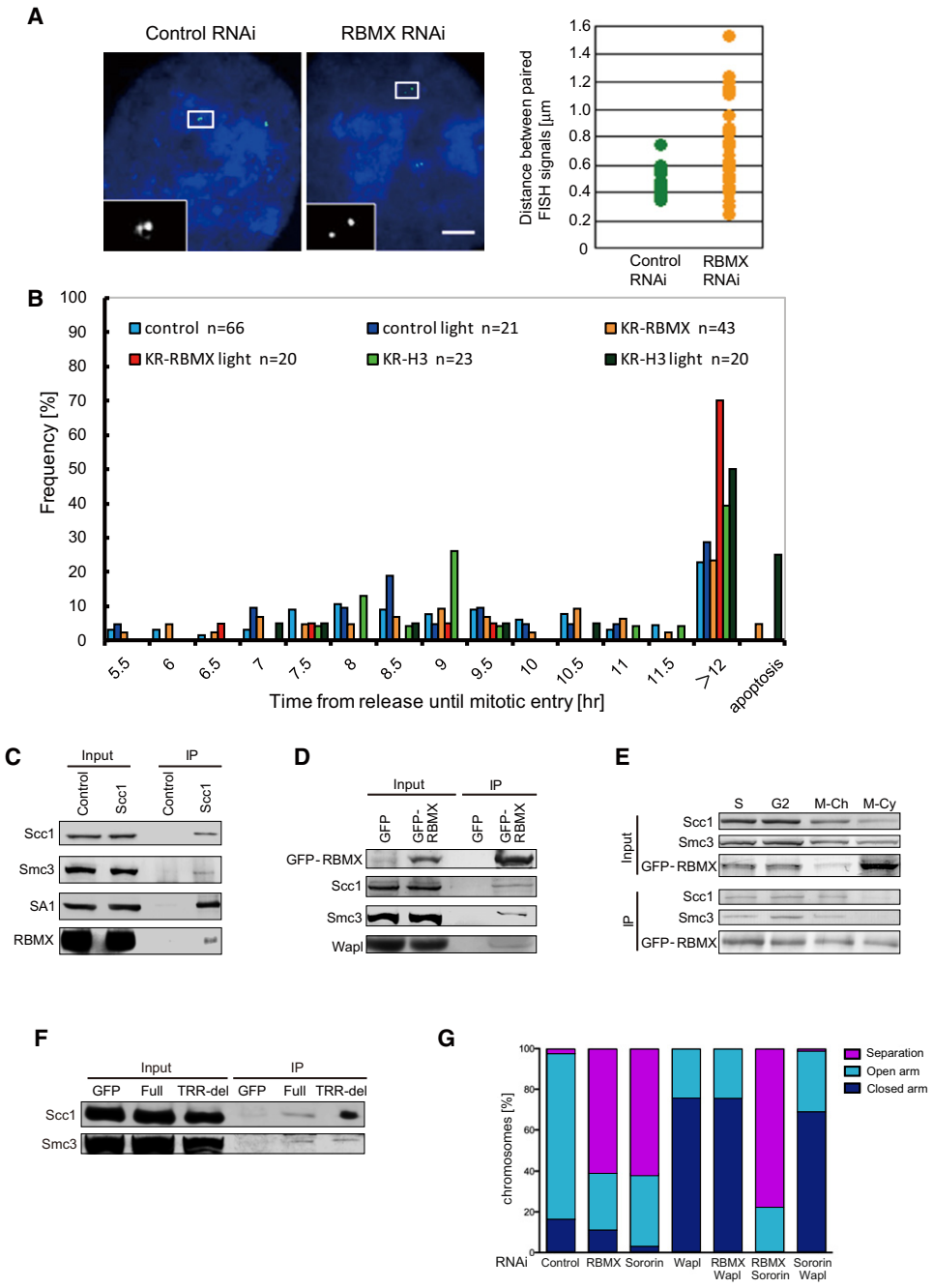

Figure 4. RBMX Is Required for Cohesion Maintenance

(A) The distance between sister chromatids was measured by FISH experiments. HeLa cells were synchronized by double-thymidine treatment. Cells were harvested 5 hr after release from the second arrest. FISH analysis using a probe specific for the trisomic *tff1* locus on chromosome 21 successfully detected two pairs of FISH signals (green) in the control and RBMX RNAi cells. DNA was counterstained with DAPI (blue). The paired signals are magnified (lower left in each image). The distance between paired FISH signals was measured. Scale bar, 5 µm.

(B) Depletion of RBMX at G2 phase activated the G2/M checkpoint. HeLa cells were synchronized by double-thymidine treatment. RBMX and histone H3 were inactivated at G2 phase by chromophore-assisted light inactivation with KillerRed fused with RBMX (KR-RBMX) and histone H3 (KR-H3). The controls are HeLa cells expressing GFP-H1.2. The control, KR-RBMX, and KR-H3 cells were irradiated with green light 5.5 hr after release from the second arrest (control light, KR-RBMX light, and KR-H3). The time of mitotic entrance was determined by detecting the nuclear envelope breakdown using live imaging based on GFP-H1.2 fluorescence.

(C) Immunoblotting was performed using immunoprecipitates from the nuclear fraction. Immunoprecipitates (IP) were obtained with Scc1 antibody (Scc1) or a control antibody and analyzed by immunoblotting with Scc1, Smc3, SA1, and RBMX antibodies. Of the IP protein amount, 1.25% was loaded for the input.

and chromatin fractions at different NaCl concentrations. RBMX was detected mainly in the chromatin fraction; this is similar to what was observed for the cohesin subunits, Scc1 and Smc3 (Figure S4A). Scc1 depletion did not influence the subnuclear localization of RBMX (Figures S4B and S4C), suggesting that RBMX can associate with chromatin in a cohesin-independent manner. Moreover, RBMX fused with the photosensitizer KillerRed, which generates reactive oxygen species upon light irradiation (Bulina et al., 2006), induced the arrest at the mitotic entrance possibly because of the activation of a G2/M checkpoint by DNA damage (Figures 4B and S4D–S4F). This result also supports the proposal that RBMX associates with chromatin.

By immunoprecipitation an association between RBMX and endogenous Scc1 was detected (Figures 4C and S4G); in addition, exogenous RBMX was found to associate with Scc1, Smc3, and the cohesin regulator, Wapl (Kueng et al., 2006) (Figure 4D). We observed that RBMX dissociated from mitotic chromosomes and was localized abundantly in the cytoplasm during mitosis (Figure 1A). The interaction between RBMX and cohesin was detected in the nuclei at G2 and S phases and was absent in the cytoplasm at M phase (Figure 4E), suggesting that at M phase there is no association between cytoplasmic RMBX and cohesin. This raises the possibility that the association of RBMX with cohesin might be an indirect interaction bridged by chromatin rather than a direct protein-protein interaction (Peters et al., 2008). To further investigate this possibility, we performed the immunoprecipitation with RBMX lacking TRR, which cannot interact with chromatin (Figures 2C and 2D). The results show that the TRR-del proteins were associated with Scc1 and Smc3 (Figure 4F), indicating that the TRR domain was not necessary for the association between RBMX and cohesin. This result suggested that RBMX associated with cohesin not through chromatin but via a protein-protein interaction. A two-hybrid interaction analysis demonstrated that RBMX could interact with other proteins through all regions except through the RRM domain (Heinrich et al., 2009). Taken together, these results imply that RBMX can interact with cohesin through the regions except the RRM and TRR domains.

At S/G2 phase, Sororin antagonizes Wapl, the regulatory protein responsible for cohesion dissolution from the cohesin complex (Nishiyama et al., 2010). To examine the functional relationships between the cohesion regulatory proteins, we performed double knockdowns of RBMX, Sororin, and Wapl (Figure 4G). The phenotype of closed arms in RBMX/Wapl double-knockdown cells was the same as the phenotype in cells with Wapl knockdown alone. This observation indicates that RBMX is required for cohesion only when there is sufficient expression of Wapl, suggesting that, in addition to Sororin, RBMX is an antagonist of Wapl. It is possible that, as a regulatory factor of cohesion, RBMX is part of the cohesin complex during the S/G2 phase to M phase transition. Moreover, the percentage of the chromosomes with the separation phenotype caused by the double knockdown of RBMX and Sororin was more than the percentage for either the RBMX or Sororin knockdowns alone (Figure 4G). This observation implies that RBMX and Sororin are involved in the regulation of cohesion through different pathways.

This report is, to our knowledge, the first to identify RBMX as a regulator of sister chromatid cohesion. We believe that this finding is an important step to understanding how chromosomes are constructed.

EXPERIMENTAL PROCEDURES

RNAi-Mediated Knockdown

We used RBMX siRNA-1 (5′-UCAAGAGGAUAUAGCGAUATT-3′) and RBMX siRNA-2 (5′-CGGAUAUGGUGGAAGUCGAUU-3′) for RBMX knockdown. The knockdowns of Aurora B, Plk1, Sororin, and Wapl were performed using gene-specific siRNAs (Takata et al., 2007a; Schmitz et al., 2007; Kueng et al., 2006). For the RBMX siRNA rescue assay, three silent mutations were introduced into the GFP-RBMX vector, changing the nucleotide sequence at position 921–932 in the RBMX gene to 5′-GGCTACAGCGAC-3′ (the italics indicate silent mutations). The RNAi-refractory constructs were transfected into HeLa cells 4 hr before transfecting them with the siRNAs. Negative control siRNA (S5C-0600) was purchased from Cosmo Bio (Tokyo).

Live-Cell Imaging and Chromophore-Assisted Light Inactivation

HeLa cells stably expressing GFP-histone H1.2 were cultured in 35 mm glass-bottom dishes (Matsunami, Osaka, Japan) and transfected with siRNA using Lipofectamine 2000 (Invitrogen, Carlsbad, CA, USA). The medium was changed to a CO_2-independent medium (Invitrogen) supplemented with 10% FBS, 100 U/ml penicillin G, 0.1 mg/ml streptomycin, 4 mM glutamine, and 20 mM HEPES (pH 7.4) 1 hr before imaging. Dishes were placed on the inverted platform of a fluorescence microscope (IX-81; Olympus, Tokyo) equipped with a CO_2 chamber set at 37°C. Fluorescence images were acquired every 3 min using a 40× objective (Olympus, PlanFLN, NA = 1.30) controlled with MetaMorph software (Universal Imaging, Burbank, CA, USA). Stacks were assembled and processed using MetaMorph software.

Chromophore-assisted light inactivation was performed using HeLa cells stably expressing GFP-histone H1.2. The cells were transfected with KillerRed (Evrogen, Moscow) fused with RBMX and synchronized with thymidine. KillerRed phototoxicity was induced by 550 nm green-light irradiation according to a previously described method (Bulina et al., 2006), 5.5 hr after the release from thymidine arrest.

(D) Immunoblotting was performed using immunoprecipitates from the nuclear fraction of HeLa cells transiently expressing GFP or stably expressing GFP-RBMX. Immunoprecipitates (IP) were obtained with GFP antibody and analyzed by immunoblotting with RBMX, Scc1, Smc3, and Wapl antibodies. Of the IP protein amount, 1.25% was loaded for the input.
(E) Immunoblotting was performed using immunoprecipitates from the nuclear fraction at S and G2 phases, the chromatin (M-ch) and cytoplasm fractions (M-cy) at M phase of synchronized cells stably expressing GFP-RBMX. Immunoprecipitates (IP) were obtained with GFP antibody and analyzed by immunoblotting with Scc1, Smc3, and GFP antibodies. Of the IP protein, 1.25% was loaded for the input.
(F) Immunoblotting was performed using immunoprecipitates from the nuclear fraction of HeLa cells transiently expressing GFP-TRR-del. Immunoprecipitates (IP) were obtained with GFP antibody and analyzed by immunoblotting with Scc1 and Smc3 antibodies. Of the IP protein, 1.25% was loaded for the input.
(G) Chromosome morphologies in knockdown cells were categorized into three groups: closed arm, chromosomes maintained sister chromatid cohesion over their entire length; open arm, sister chromatids cohered at the centromeric region, but not along the chromosome arm; and separation, sister chromatids were separated.
See also Figure S4.

SUPPLEMENTAL INFORMATION

Supplemental information includes Extended Experimental Procedures and four figures and can be found with this article online at doi:10.1016/j.celrep.2012.02.005.

LICENSING INFORMATION

ACKNOWLEDGMENTS

This study was supported by the Grant-in-Aid for Young Scientists (A) (18687005), Scientific Research (B) (20370027, 23370029) (to S.M.), Scientific Research (A) (21248040) from the Japan Society for the Promotion of Science, and Special Coordination Funds for Nano-Devices for Structural and Functional Analyses of Chromosomes (to K.F.) from the Ministry of Education, Culture, Sports, Science and Technology in Japan. Live-cell imaging analyses were supported by Grants-in-Aid from Development of Systems and Technology for Advanced Measurement and Analysis, Japan Science and Technology Agency (to S.M.).

Received: August 9, 2011
Revised: December 12, 2011
Accepted: February 9, 2012
Published online: March 22, 2012

REFERENCES

Bulina, M.E., Chudakov, D.M., Britanova, O.V., Yanushevich, Y.G., Staroverov, D.B., Chepurnykh, T.V., Merzlyak, E.M., Shkrob, M.A., Lukyanov, S., and Lukyanov, K.A. (2006). A genetically encoded photosensitizer. Nat. Biotechnol. *24*, 95–99.

Cheeseman, I.M., and Desai, A. (2008). Molecular architecture of the kinetochore-microtubule interface. Nat. Rev. Mol. Cell Biol. *9*, 33–46.

Dai, J., Sullivan, B.A., and Higgins, J.M. (2006). Regulation of mitotic chromosome cohesion by Haspin and Aurora B. Dev. Cell *11*, 741–750.

Delbridge, M.L., Lingenfelter, P.A., Disteche, C.M., and Graves, J.A. (1999). The candidate spermatogenesis gene RBMY has a homologue on the human X chromosome. Nat. Genet. *22*, 223–224.

Gambe, A.E., Ono, R.M., Matsunaga, S., Kutsuna, N., Higaki, T., Higashi, T., Hasezawa, S., Uchiyama, S., and Fukui, K. (2007). Development of a multistage classifier for a monitoring system of cell activity based on imaging of chromosomal dynamics. Cytometry A *71*, 286–296.

Giménez-Abián, J.F., Sumara, I., Hirota, T., Hauf, S., Gerlich, D., de la Torre, C., Ellenberg, J., and Peters, J.M. (2004). Regulation of sister chromatid cohesion between chromosome arms. Curr. Biol. *14*, 1187–1193.

Hauf, S., Roitinger, E., Koch, B., Dittrich, C.M., Mechtler, K., and Peters, J.M. (2005). Dissociation of cohesin from chromosome arms and loss of arm cohesion during early mitosis depends on phosphorylation of SA2. PLoS Biol. *3*, e69.

Heinrich, B., Zhang, Z., Raitskin, O., Hiller, M., Benderska, N., Hartmann, A.M., Bracco, L., Elliott, D., Ben-Ari, S., Soreq, H., et al. (2009). Heterogeneous nuclear ribonucleoprotein G regulates splice site selection by binding to CC(A/C)-rich regions in pre-mRNA. J. Biol. Chem. *284*, 14303–14315.

Ivanov, D., Schleiffer, A., Eisenhaber, F., Mechtler, K., Haering, C.H., and Nasmyth, K. (2002). Eco1 is a novel acetyltransferase that can acetylate proteins involved in cohesion. Curr. Biol. *12*, 323–328.

Kawashima, S.A., Yamagishi, Y., Honda, T., Ishiguro, K., and Watanabe, Y. (2010). Phosphorylation of H2A by Bub1 prevents chromosomal instability through localizing shugoshin. Science *327*, 172–177.

Kitajima, T.S., Sakuno, T., Ishiguro, K., Iemura, S., Natsume, T., Kawashima, S.A., and Watanabe, Y. (2006). Shugoshin collaborates with protein phosphatase 2A to protect cohesin. Nature *441*, 46–52.

Kline-Smith, S.L., and Walczak, C.E. (2004). Mitotic spindle assembly and chromosome segregation: refocusing on microtubule dynamics. Mol. Cell *15*, 317–327.

Koshland, D.E., and Guacci, V. (2000). Sister chromatid cohesion: the beginning of a long and beautiful relationship. Curr. Opin. Cell Biol. *12*, 297–301.

Kueng, S., Hegemann, B., Peters, B.H., Lipp, J.J., Schleiffer, A., Mechtler, K., and Peters, J.M. (2006). Wapl controls the dynamic association of cohesin with chromatin. Cell *127*, 955–967.

Lafont, A.L., Song, J., and Rankin, S. (2010). Sororin cooperates with the acetyltransferase Eco2 to ensure DNA replication-dependent sister chromatid cohesion. Proc. Natl. Acad. Sci. USA *107*, 20364–20369.

Losada, A. (2008). The regulation of sister chromatid cohesion. Biochim. Biophys. Acta *1786*, 41–48.

Losada, A., and Hirano, T. (2005). Dynamic molecular linkers of the genome: the first decade of SMC proteins. Genes Dev. *19*, 1269–1287.

Losada, A., Hirano, M., and Hirano, T. (2002). Cohesin release is required for sister chromatid resolution, but not for condensin-mediated compaction, at the onset of mitosis. Genes Dev. *16*, 3004–3016.

Ma, N., Matsunaga, S., Takata, H., Ono-Maniwa, R., Uchiyama, S., and Fukui, K. (2007). Nucleolin functions in nucleolus formation and chromosome congression. J. Cell Sci. *120*, 2091–2105.

Mazeyrat, S., Saut, N., Mattei, M.G., and Mitchell, M.J. (1999). RBMY evolved on the Y chromosome from a ubiquitously transcribed X-Y identical gene. Nat. Genet. *22*, 224–226.

Nasmyth, K. (2001). Disseminating the genome: joining, resolving, and separating sister chromatids during mitosis and meiosis. Annu. Rev. Genet. *35*, 673–745.

Nasmyth, K. (2002). Segregating sister genomes: the molecular biology of chromosome separation. Science *297*, 559–565.

Nasmyth, K., and Haering, C.H. (2009). Cohesin: its roles and mechanisms. Annu. Rev. Genet. *43*, 525–558.

Nishiyama, T., Ladurner, R., Schmitz, J., Kreidl, E., Schleiffer, A., Bhaskara, V., Bando, M., Shirahige, K., Hyman, A.A., Mechtler, K., and Peters, J.M. (2010). Sororin mediates sister chromatid cohesion by antagonizing Wapl. Cell *143*, 737–749.

Obuse, C., Iwasaki, O., Kiyomitsu, T., Goshima, G., Toyoda, Y., and Yanagida, M. (2004). A conserved Mis12 centromere complex is linked to heterochromatic HP1 and outer kinetochore protein Zwint-1. Nat. Cell Biol. *6*, 1135–1141.

Peters, J.M., Tedeschi, A., and Schmitz, J. (2008). The cohesin complex and its roles in chromosome biology. Genes Dev. *22*, 3089–3114.

Rivera, T., and Losada, A. (2006). Shugoshin and PP2A, shared duties at the centromere. Bioessays *28*, 775–779.

Rowland, B.D., Roig, M.B., Nishino, T., Kurze, A., Uluocak, P., Mishra, A., Beckouët, F., Underwood, P., Metson, J., Imre, R., et al. (2009). Building sister chromatid cohesion: smc3 acetylation counteracts an antiestablishment activity. Mol. Cell *33*, 763–774.

Salic, A., Waters, J.C., and Mitchison, T.J. (2004). Vertebrate shugoshin links sister centromere cohesion and kinetochore microtubule stability in mitosis. Cell *118*, 567–578.

Samanta, A., Li, B., Song, X., Bembas, K., Zhang, G., Katsumata, M., Saouaf, S.J., Wang, Q., Hancock, W.W., Shen, Y., and Greene, M.I. (2008). TGF-beta and IL-6 signals modulate chromatin binding and promoter occupancy by acetylated FOXP3. Proc. Natl. Acad. Sci. USA *105*, 14023–14027.

Schmitz, J., Watrin, E., Lénárt, P., Mechtler, K., and Peters, J.M. (2007). Sororin is required for stable binding of cohesin to chromatin and for sister chromatid cohesion in interphase. Curr. Biol. *17*, 630–636.

Soulard, M., Della Valle, V., and Larsen, C.J. (2002). Autoimmune antibodies to hnRNPG protein in dogs with systemic lupus erythematosus: epitope mapping of the antigen. J. Autoimmun. *18*, 221–229.

Sumara, I., Vorlaufer, E., Stukenberg, P.T., Kelm, O., Redemann, N., Nigg, E.A., and Peters, J.M. (2002). The dissociation of cohesin from chromosomes in prophase is regulated by Polo-like kinase. Mol. Cell *9*, 515–525.

Takata, H., Matsunaga, S., Morimoto, A., Ma, N., Kurihara, D., Ono-Maniwa, R., Nakagawa, M., Azuma, T., Uchiyama, S., and Fukui, K. (2007a). PHB2 protects sister-chromatid cohesion in mitosis. Curr. Biol. *17*, 1356–1361.

Takata, H., Matsunaga, S., Morimoto, A., Ono-Maniwa, R., Uchiyama, S., and Fukui, K. (2007b). H1.X with different properties from other linker histones is required for mitotic progression. FEBS Lett. *581*, 3783–3788.

Takata, H., Uchiyama, S., Nakamura, N., Nakashima, S., Kobayashi, S., Sone, T., Kimura, S., Lahmers, S., Granzier, H., Labeit, S., et al. (2007c). A comparative proteome analysis of human metaphase chromosomes isolated from two different cell lines reveals a set of conserved chromosome-associated proteins. Genes Cells *12*, 269–284.

Tang, Z., Shu, H., Qi, W., Mahmood, N.A., Mumby, M.C., and Yu, H. (2006). PP2A is required for centromeric localization of Sgo1 and proper chromosome segregation. Dev. Cell *10*, 575–585.

Tsend-Ayush, E., O'Sullivan, L.A., Grützner, F.S., Onnebo, S.M., Lewis, R.S., Delbridge, M.L., Marshall Graves, J.A., and Ward, A.C. (2005). RBMX gene is essential for brain development in zebrafish. Dev. Dyn. *234*, 682–688.

Tsuei, D.J., Hsu, H.C., Lee, P.H., Jeng, Y.M., Pu, Y.S., Chen, C.N., Lee, Y.C., Chou, W.C., Chang, C.J., Ni, Y.H., and Chang, M.H. (2004). RBMY, a male germ cell-specific RNA-binding protein, activated in human liver cancers and transforms rodent fibroblasts. Oncogene *23*, 5815–5822.

Uchiyama, S., Kobayashi, S., Takata, H., Ishihara, T., Hori, N., Higashi, T., Hayashihara, K., Sone, T., Higo, D., Nirasawa, T., et al. (2005). Proteome analysis of human metaphase chromosomes. J. Biol. Chem. *280*, 16994–17004.

Vagnarelli, P., Morrison, C., Dodson, H., Sonoda, E., Takeda, S., and Earnshaw, W.C. (2004). Analysis of Scc1-deficient cells defines a key metaphase role of vertebrate cohesin in linking sister kinetochores. EMBO Rep. *5*, 167–171.

Watanabe, Y. (2005). Shugoshin: guardian spirit at the centromere. Curr. Opin. Cell Biol. *17*, 590–595.

Yamagishi, Y., Sakuno, T., Shimura, M., and Watanabe, Y. (2008). Heterochromatin links to centromeric protection by recruiting shugoshin. Nature *455*, 251–255.